A spiking neuron model of biased inferential decision making

Anonymous CogSci submission

Abstract

Inferential decision making requires the coordinated interaction of anatomically and functionally distinct brain areas in cortex, subcortex, and brainstem. We study these interactions using a spiking neuron model that dynamically performs a simple, stochastic decision task in a human-like manner. The model (a) includes populations corresponding to dorsolateral prefrontal cortex, orbitofrontal cortex, inferior frontal cortex, pre-supplementary motor area, and basal ganglia; (b) is constructed using 9000 leaky-integrate-and-fire neurons with 20 million connections; and (c) realizes dedicated cognitive operations such as inferential weighing of inputs, accumulation of evidence for multiple choice alternatives, competition between potential actions, dynamic thresholding of behavior, and stress-mediated biasing of decision time. We show that model agents recreate human behavior on the task, with some agents choosing quickly but inaccurately and other choosing slowly but accurately. These results support the hypothesis that modulatory systems in the brain bias decision making towards speed or accuracy, providing valuable cognitive flexibility in real-world environments where animals must respond to dynamic and uncertain stimuli.

Keywords: Neural Engineering Framework; decision making; computational model; bias

Introduction

In inferential decision making (IDM), an agent must gather evidence about the value of possible actions then choose between them. IDM tasks pervade natural and artificial environments, presenting a unique set of cognitive challenges related to the acquisition and processing of information. Notably, these tasks are dynamic and stochastic: observing and processing sensory data takes time, and data are often sampled randomly from underlying probability distributions. To effectively solve IDM tasks like appraising a potential mate or diagnosing an illness, animals must deploy cognitive processes that deal with time and uncertainty; they must accumulate the probabilistic evidence for each potential choice, continually compare those choices them until some decision criteria is reached, and finally implement the preferred option. Although most humans perform these steps intuitively, the underlying cognitive operations are far from trivial: an agent must internally represent the sampled evidence, judge the quality of that information, remember evidence for multiple choices, and choose when to make a decision. All of this must be done flexibly to meet task demands and account for the environmental context.

We are interested in the neural and cognitive processes that underlie decision making on IDM tasks, specifically how brains manage tradeoffs between speed and accuracy. It makes evolutionary sense that, in environments where an agent must move towards desirable outcomes expediently, IDM should proceed quickly and accurately. Unfortunately, either speed (time taken before making a choice) or accuracy (about the value/validity of the choice) is often sacrificed in dynamic and uncertain environments. We believe that brains use biasing to flexibly adapt IDM processes to favor either speed or accuracy, and that individuals may adopt different strategies, either contextually or habitually, on these tasks.

Consider an IDM task in which an interviewer must decide which of four job candidates would be the most productive worker. The interviewer may call a candidate into her office, ask them a question, and numerically score their response. By repeatedly calling different candidates and asking different questions, the interviewer dynamically collects evidence about individuals' potential productivity. Each of the interviewer's questions probes one of several *attributes*, such as intelligence, initiative, or creativity. Because the interview process is imperfect, the score assigned by the interviewer to, say, a candidate's intelligence may not reflect their true intelligence: the *value* assigned to that attribute is sampled stochastically. Each attribute has an associated *validity*, which indicates the partial information it conveys about productivity and the confidence that the scoring is accurate. To decide which candidate is the most productive, the interviewer repeatedly measures one candidate's value for one attribute, multiplies this score by the attribute's validity, and integrates the result with existing evidence for the candidate. Once the interviewer has asked each candidate each question, she can select the individual with the greatest evidence; assuming that the validities are appropriate and the interviewer can do arithmetic, this process will lead to the correct selection. Although this algorithm is effective, it may be unnecessarily slow; for example, if one candidate receives a perfect score, there is no need to continue interviewing. Various heuristics could similarly improve speed, but many come at the expense of no longer guaranteeing the correct selection. Our goal is to study how the cognitive biases that realize these heuristics affect IDM in humans.

In this study, we present an anatomically mapped, spiking neuron model of the cognitive processes underlying IDM. The model performs a simplified version of the task for which human behavioral data is available. We show that manipulating model parameters governing the dynamic threshold for decision making leads to heterogeneous agent behavior and reproduces a diversity of strategies used by humans on the task. Specifically, the distribution of cues requested before making a decision is comparable in model agents and human participants. Furthermore, we observe losses in accuracy associated with faster decisions at similar levels in the model and in humans. We conclude by discussing extensions of the model to expand its cognitive realism and to account for emotional bias.

Background

Psychology

Inferential decision making with multiple cues requires many interrelated cognitive operations. Normative theories of choice rooted in economics postulate that before making a decision, humans should process all available information and carefully weigh the cues: that is, multiply validities with the cue values and add the results. Descriptive theories of choice, on the other hand, postulate that people frequently use heuristics to simplify decision problems (Gigerenzer & Todd, 1999). Although generally quite successful, heuristics trade off choice accuracy for speed, particularly in situations that require integrating many pieces of information. Given their simplicity, heuristics were proposed as plausible models of choice, particularly under time pressure (Rieskamp & Hoffrage, 2008) and stress (Wichary, Mata, & Rieskamp, 2016). Research suggests that these factors bias decision making, such that choices are made earlier and with less information, in order to adapt to urgent or demanding situations.

Neuroanatomy

Decision strategies are composed of distinct cognitive operations associated with activity in distinct brain structures. In accordance with growing literature, we assume that the following areas are responsible for the various operations required by our computational model. Ventromedial prefrontal cortex, orbitofrontal cortex (OFC), and dorsolateral prefrontal cortex (dlPFC) perform cue evaluation (weighting) (Rangel & Clithero, 2014). dlPFC is also responsible for temporary retention of cue weights in working memory and performs weighted evidence accumulation (D'Esposito, 2007). Option selection is executed by the basal ganglia (BG) and its recurrent connections to cortex (Bogacz & Gurney, 2007). Within these loops, presupplementary motor area (pSMA) and the right inferior frontal cortex (rIFC) act as gates to the striatal input nuclei of the basal ganglia (BG) (Forstmann et al., 2010), allowing action selection only once an evidence threshold has been passed (Aron, Robbins, & Poldrack, 2014). Finally, norepinephrine signals sent from the locus coeruleus (LC) to cortex may bias decision making towards speed or accuracy (Chamberlain et al., 2009) in response to time pressure or stress (Aston-Jones & Cohen, 2005). Empirical results generally support the role of these structures in complex decision making with fast choices and little information (Oh-Descher, Beck, Ferrari, Sommer, & Egner, 2017).

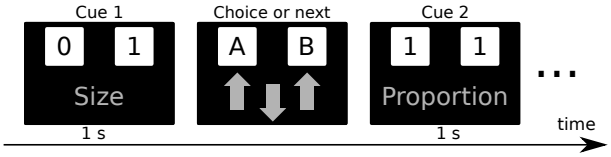

Figure 1: Demonstration of the experimental paradigm.

Task

In our IDM task (Wichary, Magnuski, Oleksy, & Brzezicka, 2017), participants begin by memorizing validities associated with six cue attributes. The validities in this task, which range from 0.706 to 0.600, are compensatory: they do not differ significantly from one another, encouraging participants to pay attention to all cue information rather than (heuristically) considering only the top few attributes. During the task, participants are simultaneously shown the values (0 or 1) of objects *A* and *B* for one attribute (see Fig. 1). The participants respond by pressing one of three buttons, indicating their selection of *A*, selection of *B*, or a request for more information. If they choose the later, the current display is replaced by another pair of values for the next attribute. This is repeated until the participant makes a choice or until all attributes have been exhausted, at which point a choice is forced. Attributes are presented in order of highest-to-lowest validity. Participants are not provided feedback on whether their final choice was correct. This task is repeated 48 times; behavior on each trial is quantified by the number of cues requested before the final decision and whether the choice corresponded to the highest-value option.

Neural Engineering Framework

The NEF (Eliasmith & Anderson, 2003) describes how spiking neural activity may represent a time-varying, vector-valued signal $\mathbf{x}(t)$ such as value, validity, or evidence. A neuron spikes most frequently when presented with its particular "preferred stimulus" and responds less strongly to increasingly dissimilar stimuli (i.e. values of $\mathbf{x}(t)$). In the NEF, each neuron i is accordingly assigned a preferred direction vector, or *encoder*, $\mathbf{e}_i$. To produce a variety of tuning curves and firing rates that match electrophysiological variance within the brain, each neuron is also assigned a unique gain α_i and bias β_i. These quantities determine how strongly an incident vector $\mathbf{x}(t)$ drives the neuron:

$$I_{in}(t) = \alpha_i * (\mathbf{e_i} \cdot \mathbf{x}(t)) + \beta_i \quad (1)$$

where $I_{in}(t)$ is the current flowing into the neuron and $(\cdot)$ is the dot product between the encoder and input vector. So long as there is a well-defined relationship between input current and resulting firing rate, the neuron's activity can be said to encode the vector $\mathbf{x}(t)$. A distributed encoding extends this

notion: if $\mathbf{x}(t)$ is fed into multiple neurons, each with a unique tuning curve defined by $\mathbf{e}$, α, and β, then each neuron will respond with a unique spiking pattern $a_i(t)$, and the collection of all neural activities will robustly encode the signal.

For neural encoding to be meaningful, there must be methods to recover, or decode, the original vector from the neurons' activities; together, encoding and decoding constitute neural *representation*. The NEF identifies neural *decoders* $\mathbf{d}_i$ that either perform this recovery or compute arbitrary functions, $f(\mathbf{x})$, of the represented vector. A functional decoding with $\mathbf{d}_i^f$ allows networks of neurons to *transform* the signal into a new state, which is essential for performing operations such as value-validity multiplication. To compute these transformations, a linear decoding is applied to the activities of the neural population:

$$\hat{f}(\mathbf{x}(t)) = \sum_{i=0}^{n} a_i(t) * \mathbf{d}_i^f, \tag{2}$$

where n is the number of neurons and the hat notation indicates that the computed function is an estimate. To find decoders $\mathbf{d}_i^f$ that compute the desired function, we use least-squares optimization to minimize the error between the target value $f(\mathbf{x}(t))$ and the decoded estimate $\hat{f}(\mathbf{x}(t))$. The general-purpose Nengo neural simulator (Bekolay, Laubach, & Eliasmith, 2014) includes methods to optimize these decoders for the specified transformations. Connection *weights* between each presynaptic neuron i and each postsynaptic neuron j combine encoders and decoders into a single value used during simulation

$$w_{ij} = \alpha_j \mathbf{e}_j \cdot \mathbf{d}_i^f. \tag{3}$$

Finally, the NEF specifies methods to build neural networks that implement any dynamical system, including linear systems of the form $\dot{\mathbf{x}}(t) = A\mathbf{x}(t) + B\mathbf{u}(t)$. To do so, the matrices A and B must be modified to account for the dynamics that naturally occur when using neurons with non-instantaneous synapses. Nengo performs this optimization for the specified target dynamics; this is essential for constructing networks that include the recurrent connections required for working memory, evidence accumulation, and choice competition.

Model

The model architecture is summarized in Fig. 2 and outlined here, with detailed descriptions of key components in the following paragraphs. A two-dimensional vector representing the values of A and B for the currently displayed attribute is provided as external input to a population labelled **OFC**. This population also receives the "remembered" cue validities; we choose to model this recall process as a noisy perturbation of externally-supplied validities[1]. Neurons in **OFC** thus represent both the perceived cue value and the remembered validity for the current attribute. Connection weights between **OFC** and **dlPFC** multiply values by validities and send the result to the two-dimensional **dlPFC** population. Recurrent

[1]Imperfect recall was realized by adding a smoothed 10Hz bandpass-limited white noise signal with RMS = 0.05

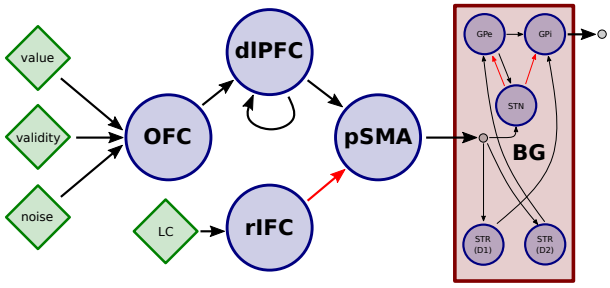

Figure 2: Model Schematic. Green diamonds are external inputs, blue circles are spiking neuron populations, and the red box is the **BG** network. Red connections are inhibitory. See text for details on represented quantities and cognitive operations.

connections within **dlPFC** implement integration, leading to the accumulation of evidence from **OFC** as additional cues are presented. When the difference between accumulated evidence for A and B exceeds a dynamic threshold, neurons in **rIFC** disinhibit the **pSMA** population. This allows information to flow from **dlPFC** to the **BG** network, where mutual inhibitory competition selects the option with the greatest evidence as a final output. If **BG** does not output a selection after one second of value/validity input, then the next cue is presented for one second, and so on.

The **dlPFC** population is a neural *integrator*, a system which maintains its currently represented value while additively incorporating any inputs. This network has previously been used in neural models of working memory, where it has reproduced activity in PFC and behavior on several WM tasks (Eliasmith, 2013). The system is described by the target dynamics $\dot{\mathbf{x}} = B\mathbf{u}$; notice that changes in the represented value $\dot{\mathbf{x}}$ do not depend on the represented value $\mathbf{x}$ itself, but only on the input $\mathbf{u}$. This implies that the integrator will remember the current evidence perfectly, and steadily add any input evidence to arrive at a new value. However, because the integrator is implemented in noisy spiking neurons, the feedforward and recurrent connections do not perfectly implement these dynamics: added evidence is slightly distorted, and memory will decay given enough time.

The **rIFC** population determines when the accumulated evidence is sufficient to make a decision. Functional connections between **dlPFC** and **rIFC** deliver the input

$$\mathbf{u}_{\text{evidence}}(t) = |E_A - E_B|, \tag{4}$$

the absolute difference in accumulated evidence for A vs B, into the latter population. Neurons in **rIFC** are initialized such that all tuning curves have (a) negative slope (larger inputs $\mathbf{u}$ produces less firing) and (b) intercepts fixed at T_{int} (inputs larger than $\mathbf{u} = T_{\text{int}}$ are rectified, producing zero activity). Together, these constraints ensure that neural activities remain positive for $\mathbf{u} < T_{\text{int}}$ and go silent for $\mathbf{u} > T_{\text{int}}$. **rIFC** connects to **pSMA** with strong inhibitory connections, such that any activity in **rIFC** dampens all activity in **pSMA**, restricting the

flow of information to **BG**. When **u** surpasses the threshold, disinhibition lifts this gating, and a decision follows shortly thereafter. Large T_{int} thus implies that the difference in accumulated evidence for A and B must be large before a selection is made.

To simulate time pressures and heuristics that favor speed over accuracy, we model an additional input $\mathbf{u}_{\text{decay}}$ to **rIFC**. This input is additive with $\mathbf{u}_{\text{evidence}}$ and grows linearly during the course of the trial

$$\mathbf{u}_{\text{decay}}(t) = T_{\text{decay}} * t, \tag{5}$$

effectively decreasing T_{int} as more cues are presented. Large T_{decay} thus implies that the decision threshold shrinks more quickly as time progresses. $\mathbf{u}_{\text{decay}}$ is also set to a large positive value when $t > 5.5$s, which removes gating at the end of the trial and forces a selection.

The **BG** population is based off an anatomical reconstruction the basal ganglia and implements winner-take-all competition between action alternatives (Stewart, Choo, & Eliasmith, 2010). As with the neural integrator, this network has been used in numerous functional brain models as part of the action selection system (Eliasmith, 2013). Here, it is simply used to select the action with the greater evidence value, effectively amplifying differences between E_A and E_B to produce a clear distinction for downstream systems. We sample the outputs of **BG** and mathematically determine which of the three action options (choose A, choose B, request more) is greater, assuming their difference surpasses a noise threshold of $T_{\text{noise}} = 0.1$.

Each model agent is initialized with unique T_{int}, T_{decay}, and random seed for generating neurons parameters **e**, α, and β. As with human participants, model agents repeat the task 48 times, and the number of cues and correctness on each trial are recorded.

Results

To clarify the dynamics of the model and investigate the causes of correct and incorrect choices, we begin by looking at time series for the state variables represented in neural populations. Fig. 3 shows three trials from different agents, including one successful choice and two failures. In the first trial (top), choice B has positive values for the first three cues, while choice A has zero value. The difference in accumulated evidence steadily grows (blue vs. red line) until the dynamic decision threshold is reached around $t = 2$s. At this point, inhibition from **LC** begins quieting the tonically active threshold population **rIFC** (black line). Once this activity decays to zero ($t = 2.5$s), the **pSMA** gate (dot-dash line) becomes disinhibited, and information flows from **dlPFC** to **BG**, which quickly selects the dominant choice. At the end of the third cue ($t = 3$s), an external check registers that **BG** has made a selection, and the agent is said to have chosen after three cues.

In the second trial (middle), both A and B have positive values, making the two choices barely distinguishable. The difference in accumulated evidence never exceeds the agent's large threshold. At $t = 5.5$s, **rIFC** is externally inhibited, opening the gate and effectively forcing a decision. By this point, noise-induced errors have accumulated in the **dlPFC** representation; when this evidence is fed to the **BG**, the agent incorrectly estimates that A's evidence exceeds B's, and it selects the wrong choice. In the third trial, the evidence initially favors B; because this agent has a small threshold, its decision criteria is met by $t = 3$, leading to selection of B. However, the remaining evidence from cues four through six tip the balance in favor of A, making the agent's early choice ultimately incorrect.

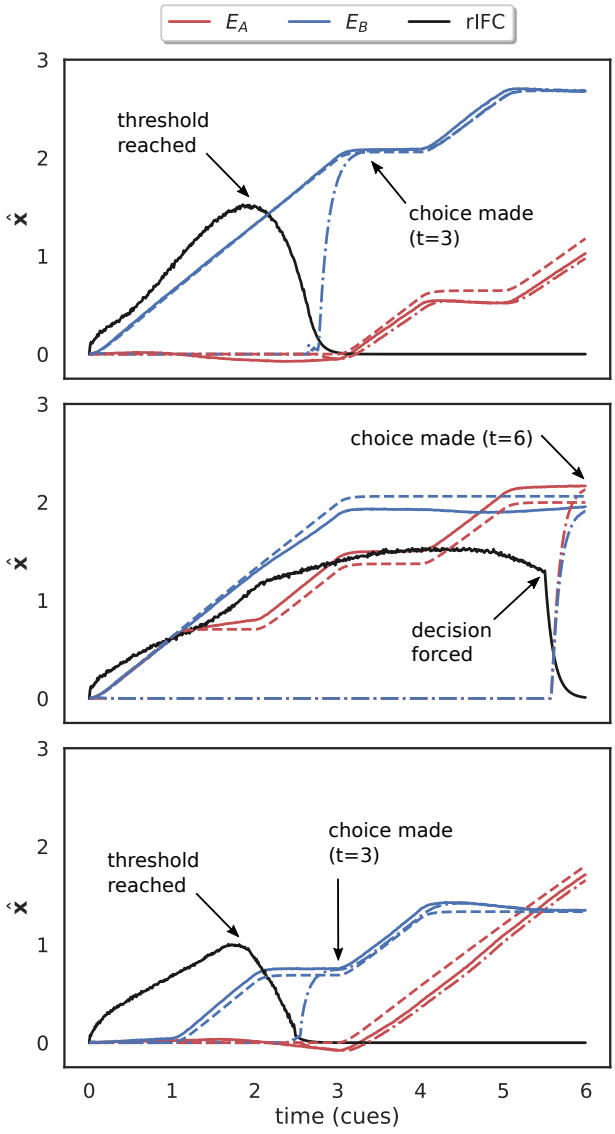

Figure 3: Time series of neural representations $\hat{\mathbf{x}}(t)$ in three model agents. Solid lines represent accumulated evidence computed by **dlPFC** neurons in the model, while dashed lines represent the ideal accumulation (included for viewing purposes). Dot-dash lines represent information flowing through the **pSMA** gate, which opens when the thresholding population **rIFC** (black line) has been inhibited.

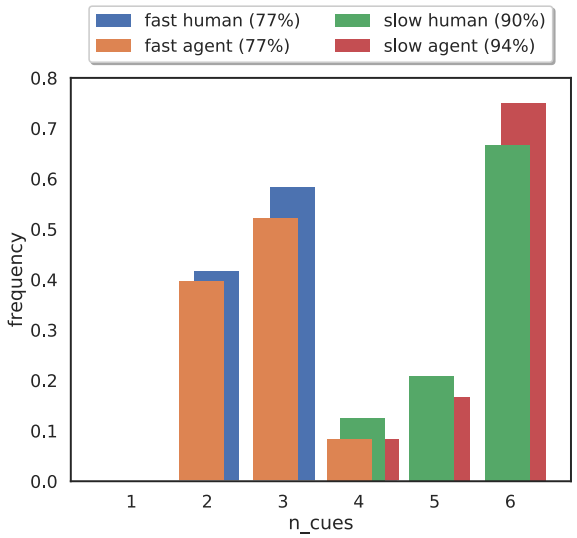

Figure 4: Behavioral distributions for humans and agents.

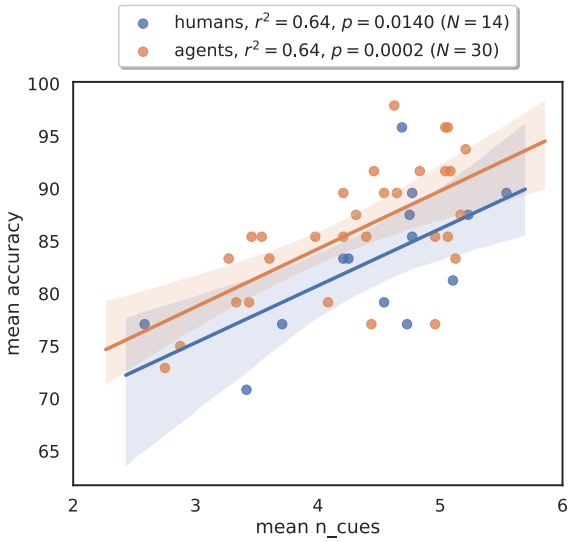

Figure 5: Mean accuracy as a function of mean cues requested.

What is an appropriate decision threshold to ensure both accuracy and speed? To answer this question, we examine individuals (both humans and agents) who strongly favor either speed or accuracy. We initialized a population of agents with random default thresholds, threshold decays, and neuron parameters, then had them perform 48 trials of our IDM task. Fig. 4 compares the behavior of fast, inaccurate decision makers and slow, accurate decision makers; behavior is quantified by plotting the number of cues inspected before a decision across all trials. As expected, an agent with small default threshold ($T_{\text{int}} = 1.41$) and large threshold decay ($T_{\text{decay}} = 0.41$) typically make selections after two or three cues, but has lower accuracy (77%) than a large default, small decay agent ($T_{\text{int}} = 3.00$, $T_{\text{decay}} = 0.33$), who views four or more cues before making a choice (accuracy 94%). The behavioral distributions and accuracies of both agents are closely aligned with relevant human participants.

The relationship between speed and accuracy is readily apparent in Fig. 5, which plots individuals' mean accuracies as a function of their mean cue requests. The trend is clear and intuitive: spending more time gathering information and performing active inference leads to more correct choices. The highest accuracies are obtained by individuals who wait for five or six cues before making a choice, although performance rarely surpasses 90% due to the difficulty of remembering and summing non-compensatory cues to high accuracy. Still, even the hastiest decision makers, who choose before the fourth cue, have accuracies above 70%, making these strategies a viable alternative when faced with strong time pressures. As before, trends in the simulated data agree with the empirical data.

Discussion

Our IDM model was designed to recreate the anatomy and cognitive function of the human decision making system using populations of spiking neurons. Although the human decision making system is too complex to capture in a simple network, we believe that our computational model distills many of its core features into a functionally-clear circuit. **OFC** receives inputs from sensory and memory systems and passes it to **dlPFC**, which performs multiplication. The result is incorporated into actively maintained representations of the evidence for various choice alternatives; such a working memory is also realized in **dlPFC**. Connections between **dlPFC** and **BG** are responsible for forwarding the utility of action alternatives to an action selection system, but these connections are gated by intermediate cortical-subcortical structures like the **pSMA**, ensuring that the individual waits until an appropriate moment to enact a behavior. Only once a controllable threshold, represented in cortical areas like the **rIFC**, has been exceeded will **BG** be freed to make a final decision and implement a motor response. This thresholding may be affected by subcortical modulation, including noradrenergic projections from **LC**, which assess environmental context, time pressures, and the individual's emotional state before deciding whether to bias decision making towards speed or accuracy. Although the particular functions computed on neural connections in our model are specific to this IDM task, we believe that this architecture may be utilized for a variety of decision making tasks involving dynamic inference on stochastic evidence.

We showed that our model agents reproduced two measures of human behavior: the number of cues examined before making a decision, and the relationship between accuracy and number of examined cues. We found that agents with smaller dynamic thresholds chose quickly but inaccurately,

while agents with larger thresholds chose slowly but with higher accuracy. The distributions of simulated choices among model agents matched both extremes of human behavior, and the trendline of speed versus accuracy across a variety of agents matched behaviors from a small human dataset. These successes suggest that the model may capture key functional aspects of the decision making apparatus in humans, especially how biases towards speed or accuracy, either situational or ingrained, may change behavior.

Future work can profitably proceed in several directions. To increase the model's cognitive realism, an associative memory system could be trained by pairing "keys" for the input attributes (unique high-dimensional vectors representing each verbally-defined attribute) with sensory inputs describing the cues' validities (one-dimensional values). This pre-training would utilize an encoder-based learning rule that has previously been used in Nengo models of associative memory (Voelker, Crawford, & Eliasmith, 2014). After training, presentation of the cue would elicit noisy recall of the associated validities, which would then be routed to **OFC** as in the current model. We are also interested in extending the model to more complex IDM tasks, including the "job interview" task described in the introduction. This task involves more choice alternatives and a wider range of cue validities; it also requires participants to view values/validities for one option at a time, and allows them to chose which option/attribute to query. This freedom introduces an extra dimension of exploration, in which the decision about which "questions to ask" may interact in interesting ways with the current evidence for various options. Finally, experimental data is available for a variant of this task in which participants were shown neutral or aversive images before performing the task, priming them with an emotional state that affected their decision making (Wichary et al., 2016). We would like to investigate whether shifts in the dynamic threshold can capture this emotional biasing, specifically whether valenced arousal states bias individuals towards faster, less accurate decision processes.

References

Aron, A. R., Robbins, T. W., & Poldrack, R. A. (2014). Inhibition and the right inferior frontal cortex: one decade on. *Trends in cognitive sciences*, *18*(4).

Aston-Jones, G., & Cohen, J. D. (2005). An integrative theory of locus coeruleus-norepinephrine function: adaptive gain and optimal performance. *Annu. Rev. Neurosci.*, *28*.

Bekolay, T., Laubach, M., & Eliasmith, C. (2014). A spiking neural integrator model of the adaptive control of action by the medial prefrontal cortex. *The Journal of Neuroscience*, *34*(5).

Bogacz, R., & Gurney, K. (2007). The basal ganglia and cortex implement optimal decision making between alternative actions. *Neural computation*, *19*(2).

Chamberlain, S. R., Hampshire, A., Müller, U., Rubia, K., Del Campo, N., Craig, K., ... others (2009). Atomoxetine modulates right inferior frontal activation during inhibitory control: a pharmacological functional magnetic resonance imaging study. *Biological Psychiatry*, *65*(7).

D'Esposito, M. (2007). From cognitive to neural models of working memory. *Philosophical Transactions of the Royal Society B: Biological Sciences*, *362*(1481).

Eliasmith, C. (2013). *How to build a brain: A neural architecture for biological cognition*. Oxford University Press.

Eliasmith, C., & Anderson, C. H. (2003). *Neural engineering: Computation, representation, and dynamics in neurobiological systems*. MIT press.

Forstmann, B. U., Anwander, A., Schäfer, A., Neumann, J., Brown, S., Wagenmakers, E.-J., ... Turner, R. (2010). Cortico-striatal connections predict control over speed and accuracy in perceptual decision making. *Proceedings of the National Academy of Sciences*, *107*(36).

Gigerenzer, G., & Todd, P. M. (1999). Fast and frugal heuristics: The adaptive toolbox. In *Simple heuristics that make us smart.* Oxford University Press.

Oh-Descher, H., Beck, J. M., Ferrari, S., Sommer, M. A., & Egner, T. (2017). Probabilistic inference under time pressure leads to a cortical-to-subcortical shift in decision evidence integration. *NeuroImage*, *162*.

Rangel, A., & Clithero, J. A. (2014). The computation of stimulus values in simple choice. In *Neuroeconomics.* Elsevier.

Rieskamp, J., & Hoffrage, U. (2008). Inferences under time pressure: How opportunity costs affect strategy selection. *Acta psychologica*, *127*(2).

Stewart, T. C., Choo, X., & Eliasmith, C. (2010). Dynamic behaviour of a spiking model of action selection in the basal ganglia. In *Proceedings of the 10th international conference on cognitive modeling.*

Voelker, A. R., Crawford, E., & Eliasmith, C. (2014). Learning large-scale heteroassociative memories in spiking neurons. *Unconventional Computation and Natural Computation*, *7*.

Wichary, S., Magnuski, M., Oleksy, T., & Brzezicka, A. (2017). Neural signatures of rational and heuristic choice strategies: a single trial erp analysis. *Frontiers in human neuroscience*, *11*.

Wichary, S., Mata, R., & Rieskamp, J. (2016). Probabilistic inferences under emotional stress: how arousal affects decision processes. *Journal of Behavioral Decision Making*, *29*(5).